Akt activator SC79 stimulates antibacterial nitric oxide production from human nasal epithelial cells and increases macrophage phagocytosis *in vitro*

Robert J. Lee,[1,2,3] Nithin D. Adappa,[1] and James N. Palmer[1]

[1]Department of Otorhinolaryngology, University of Pennsylvania Perelman School of Medicine
[2]Department of Physiology, University of Pennsylvania Perelman School of Medicine
[3]To whom correspondence should be addressed: rjl@pennmedicine.upenn.edu

Abstract

The role of the Akt serine/threonine kinase family in airway innate immunity is relatively unstudied compared with other pathways. Akt can phosphorylate and activate the endothelial nitric oxide synthase (eNOS) isoform expressed in airway epithelial cell ciliated cells. NO production by nasal epithelial cells often has antibacterial and antiviral effects. Increasing nasal epithelial NO production may be a useful anti-pathogen strategy for respiratory infections in diseases like chronic rhinosinusitis. We hypothesized that a small molecule Akt activator, SC79, might induce nasal epithelial cell NO production with bactericidal effects. We tested this in primary nasal epithelial cells isolated from residual surgical material and grown at air-liquid interface. Live cell imaging of an NO-sensitive fluorescent dye revealed that SC79 induced dose-dependent NO production. Pharmacology and gene knockdown revealed that this NO production is dependent on eNOS and Akt. The NO produced was released into the airway surface liquid and was sufficient to kill both lab and clinical strains of *P. aeruginosa* in a co-culture bacterial killing assay. Finally, because macrophages use NO signaling to enhance phagocytosis, we tested effects of SC79 in human monocyte-derived macrophages. SC79 enhanced bacterial phagocytosis in a NO-dependent and Akt-dependent manner. No overt toxicity (LDH release) or inflammatory effects (IL8 transcription) were observed in nasal cells or macrophages over 24 hrs. Together, these data suggest that multiple innate immune pathways might be stimulated by SC79 delivered via topical nasal rinse or spray. Activating Akt using SC79 or another compound might have beneficial antipathogen effects in respiratory infections.

Conflicts of interest: The authors declare no conflicts of interest.

Introduction

Generation of nitric oxide (NO) is an important airway defense mechanism. NO directly kills or inactivates bacteria and fungi by damaging their cell walls or DNA (1-5). NO also inhibits replication of influenza, parainfluenza, rhinovirus (6), and SARS-COV1 & 2 viruses (7-10). NO is generated by the enzymatic conversion of the amino acid L-arginine to L-citrulline by NO synthase (NOS). In healthy nasal ciliated cells, endothelial NOS (eNOS) is the main NOS isoform, constitutively expressed (11-13) and apically localized to the cilia base or within the cilia body itself (14-18). In endothelial cells, activation of eNOS can occur either by Ca^{2+}/calmodulin binding to eNOS or by kinase phosphorylation of eNOS at key residues like S1177 (19, 20).

We previously showed that bitter taste receptors (taste family 2 receptors, or T2Rs) activate eNOS in airway cilia (21, 22). T2Rs are G-protein coupled receptors (GPCRs) originally identified on the tongue (23) but also found in airway motile cilia (**Fig. 2A-B**) (24-28). Cilia-localized T2Rs detect bacterial metabolites (e.g., acyl-homoserine lactones (29) and quinolones (27) from *Pseudomonas*) and activate rapid (within minutes) Ca^{2+}-dependent eNOS activation to produce NO. This NO both increases cilia beating to clear bacteria and can directly kill bacteria (25, 29, 30). Macrophage-expressed T2Rs enhance phagocytosis in response to bacterial metabolites through a similar Ca^{2+} and eNOS signaling pathway (31). Thus, increasing NO generation may be useful in multiple types of cells involved in airway defense.

However, not everyone can generate NO via T2Rs, and this appears to have detrimental clinical results. Approximately 25% of people are homozygous for the *TAS2R38* AVI polymorphism, which encodes a non-functional T2R38 receptor, one of the most highly expressed T2R isoforms in sinonasal cilia. AVI/AVI individuals are more susceptible to gram-negative upper respiratory infection (25) and chronic rhinosinusitis (CRS) (32, 33). AVI/AVI individuals have poorer sinus surgical outcomes than patients homozygous for PAV (functional) T2R38 (34). This was supported by genome-wide association studies of *TAS2R38* (35, 36) and a study showing AVI/AVI patients have increased sinonasal bacteria (37). AVI T2R38 may also be detrimental in cystic fibrosis patients (38, 39).

We hypothesize that boosting epithelial NO production by nasal cells is a potential complementary strategy to treat upper respiratory infections, reducing the pressures for single agent resistance in chronic rhinosinusitis (40-43). One pathway to activate eNOS, largely unexplored in airway cell physiology, is the Akt kinase pathway. There are three mammalian Akt isoforms (Akt1, 2, and 3), which vary in tissue expression. We found that primary nasal cells grown at air liquid interface (ALI) express all three isoforms (44). Once activated, Akt can

phosphorylate multiple downstream targets like other kinases or transcription factors (45, 46), including many proteins associated with cell survival and proliferation (46, 47). Another target of Akt is eNOS. AKT phosphorylation of eNOS at S1177 can activate eNOS NO production (19, 20). We hypothesize that the NO production driven by Akt in nasal epithelial cells, like the NO produced during T2R stimulation, may enhance bacterial killing or inactivate viruses. The data below are an *in vitro* pilot study to determine if targeting the Akt pathway might be beneficial by enhancing innate immune responses during upper respiratory infections. As a model, we used both primary human nasal epithelial cells as well as primary human monocyte-derived macrophages.

Results

We tested direct Akt activation using small molecule Akt activator SC79. SC79 binds to Akt to promote a conformational change allowing Akt phosphorylation by upstream kinases (48-52). SC79 activation of Akt has beneficial effects in models of neuronal (50, 51) and hepatic disease (52). In A549 lung cancer cells, 16HBE immortalized bronchial epithelial cells, and primary nasal epithelial cells, we found that SC79 acutely increased Akt phosphorylation at S473 (44). The resulting Akt activation caused translocation of the transcription factor Nrf-2 to the nucleus, reducing NFκB-driven IL-8 transcription during co-stimulation with TNFα or toll like receptor 5 (TLR5) agonist flagellin (**Figure 1A**) (44). We also observed that SC-79 increased eNOS phosphorylation at S1177 and stimulated NO production in A549 cells (**Figure 1B**) (44), though the consequence of this NO production were not determined. To further test the effects of SC79 and downstream NO production, we first focused on primary nasal epithelial cells isolated from residual surgical material and cultured at air-liquid interface (ALI), which induces formation of motile cilia and goblet cells (**Figure 1C**), mimicking the in vivo nasal epithelium better than submerged cultures or cell line models (53, 54).

We loaded human nasal ALIs with reactive nitrogen species (RNS) indicator DAF-FM to track NO production. SC79 dose-dependently increased DAF-FM fluorescence over >10 min (**Figure 2A**). The DAF-FM fluorescence increases were blocked by NOS inhibitor L-NAME but not by inactive analogue D-NAME (**Figure 2B**). DAF-FM fluorescence changes were also blocked by NO scavenger cPTIO (**Figure 2B**). DAF-FM fluorescence changes were also blocked by siRNA directed against eNOS but not against the neuronal NOS (nNOS) isoform (**Figure 2C**). These data confirm that SC79 stimulates NO production in primary nasal cells via eNOS.

We tested if the SC79-activated NO production required Akt. We found that SC79-stimulated DAF-FM fluorescence increases were inhibited by Akt inhibitors GSK690693 and MK2206 (**Figure 3A**). DAF-FM fluorescence increases were also blocked by LY294002 (**Figure 3A**), and inhibitor of PI3 kinase (PI3K) upstream of Akt. We previously found that SC79 induced Akt phosphorylation requires PI3K (44). The SC79-induced DAF-FM fluorescence increases were also blocked by Akt inhibitor API-2 but not protein kinase C inhibitor Gö6983 (**Figure 3B**). DAF-FM fluorescence increases were also not blocked by phospholipase C inhibitor U73122 or its inactive analogue U73343 (**Figure 3C**). Together, these data suggest that SC79-stimulated eNOS activation is due to Akt and not activation of another kinase.

We previously showed that SC79 had no toxic effects on cell metabolism or proliferation

at 24 and 48 hours (44). To further test if acute SC79 stimulation had any toxic effects on primary nasal cells, we treated ALIs with SC79 for 24 hours and saw neither LDH release (via colormetric assay; **Figure 4A**) nor IL-8 production (by qPCR; **Figure 4B**). With this lack of overt toxic effects with acute treatment, we hypothesized that short-term stimulation with SC79 might be useful to activate bactericidal NO production by nasal epithelial cells. To test if the NO produced during SC79 treatment entered the airway surface liquid (ASL), we used an assay to measure ASL NO using cell-impermeant RNS-sensitive dye DAF-2 overlayed in a small volume on top of the ALI cultures (22). ASL DAF-2 fluorescence increased dose-dependently with SC79, and this was inhibited by NOS inhibitor L-NAME (**Figure 5A**). We also saw that ASL NO was not different in *TAS2R38* PAV/PAV vs AVI/AVI cultures, confirming that SC79 effects were independent of *TAS2R38* status and likely independent of T2R signaling (**Figure 5B**).

Is this NO bactericidal? To test this, we used a bacterial killing assay in which nasal ALIs kill *P. aeruginosa* in an NO-dependent fashion (22, 25) with *TAS2R38* AVI/AVI (non-functional) ALIs, which do not respond to endogenous bacterial acyl-homoserine lactones or quinolones that activate T2R38. With no exogenous stimulation, AVI/AVI exhibit minimal bacterial killing in this assay (25). Bacteria were incubated with nasal ALIs for 2 hours, and collected and stained for live (Syto9) and dead (propidium iodide [PI]) bacteria. Lab *P. aeruginosa* strains PAO-1 and ATCC27853 were used along with clinical CRS isolates P11006, 2338, and L3847. SC79 stimulated dose-dependent killing (decreased Syto9/PI fluorescence ratio) of PAO-1 and ATCC27853 in an L-NAME-sensitive and MK2206-sensitive manner (**Figure 5C**). SC-79 also stimulated killing of clinical isolates (**Figure 5C**). Antibacterial effects were confirmed by counting CFUs, and less *P. aeruginosa* were recovered from AVI/AVI nasal ALIs treated with SC79 vs ALIs treated with vehicle (0.1% DMSO) only (**Figure 6A-B**). Overall, these results suggest SC79 can stimulate nasal epithelial cells to produce bactericidal levels of NO *in vitro*.

To further determine if beneficial immune responses might be observed, we tested if SC79 enhanced macrophage phagocytosis. Macrophages are important players in early airway innate immunity (55, 56). T2R bitter taste receptors expressed in macrophages can also stimulate phagocytosis via NO signaling (31). We cultured and differentiated human macrophages from healthy apheresis donors and measured phagocytosis of FITC-labled *Escherichia coli* bioparticles (**Figure 7A**) with fluorescence read on a plate reader. SC79 increased macrophage phagocytosis in a manner inhibited by AKT inhibitors MK2206 and GSK690693 as well as NOS inhibitor L-NAME (**Figure 7B**). SC79 stimulated macrophage phagocytosis was also confirmed by a plate reader assay of *Staphylococcus aureus* labeled

with pH-sensitive dye pHrodo (Figure 7C), suggesting increased phagocytosis with SC79 and inhibition by MK2206. No LDH release was observed from macrophages over 8 hours stimulation with SC79, suggesting no overt toxic effects (**Figure 7C**). SC79-stimulation of phagocytosis of *S. aureus* was also confirmed by direct microscopy visualization and quantification, showing dose dependent effects of SC79 at 1 and 10 µg/ml (**Figure 7E-F**).

Discussion

Our data suggest that activation of Akt may have acute antibacterial effects in the nasal epithelium by activating NO production. The nose is the “front line” of respiratory defense, where host-pathogen interactions occur with every breath (57). Failure of upper respiratory defenses can lead to microbial overload and chronic rhinosinusitis (CRS), a complex syndrome of sinonasal infection and/or inflammation affecting >35 million Americans. CRS creates an aggregated direct healthcare cost of ~$8 billion annually (58), with indirect costs (e.g., missed workdays and decreased productivity) adding to the >$20 billion socioeconomic burden (58). Importantly, conventional management of acute and chronic rhinosinusitis accounts for nearly 20% of adult antibiotic prescriptions (58), making CRS a major contributor to the antibiotic resistance crisis, called “arguably the greatest risk…to human health” by the World Economic Forum (59). As the prevalence of resistance increases, conventional CRS therapies are becoming less effective (43, 60, 61). Stimulating endogenous host defenses is an attractive alternative stragey to boost immunity without the pressures for single-agent resistance.

While it is likely that one or more of the three Akt isoforms play an important role in every cell type in the body, Akt signaling is understudied in the context of airway innate immunity or airway epithelial physiology in general. The role of Akt in innate defense is unclear, even despite the fact that Akt is downstream of several toll-like receptors (62, 63). The study of Akt’s role is complicated by cross talk between multiple convergent signaling pathways that are activated downstream of TLRs and other receptors. We previously examined Akt signaling in airway cells using SC79 to directly activate Akt in the absence of other kinases (44), and interestingly found anti-inflammatory effects of SC79 Akt activation due to Nrf2 upregulation and translocation to the nucleus (44). Here, we show that the NO produced during SC79 stimulation of primary nasal ALIs is Akt-dependent and sufficient to kill bacteria. It may also be sufficient to inactivate viruses or fungi, but further testing is needed. SC79 also enhanced macrophage phagocytosis via an Akt-dependent and NO-dependent mechanism. Thurs, we hypothesize that SC79 delivered topically in a nasal spray or rinse might be effective against some types of upper respiratory infections by stimulating endogenous NO production.

While NO donors are being actively explored for CRS (64, 65), we hypothesize that a useful alternative strategy is to target endogenous signaling pathways to generate more physiological levels of NO production. An example of this is the cilia T2R-dependent pathway (28). When this pathway has reduced function (in *TAS2R38* AVI/AVI patients), several measures of CRS disease severity are worsened (32, 39, 66-68). One strategy to overcome this is to use T2R agonists like quinine (69) or diphenhydramine derivatives (70) that might activate

T2Rs in cilia beyond T2R38. Yet another strategy, explored here, is using a compound like SC79 that signals to eNOS via a completely different mechanism (Akt vs Ca^{2+}/calmodulin signaling). We believe that the above results comprise pilot data suggesting Akt activation should be further explored as a non-antibiotic antimicrobial strategy in the context of respiratory infections in CRS and possibly other airway diseases.

Notably, Akt plays a central role in cell growth and metabolism (46). An important caveat to activating Akt hinges on the central role that the PI3K-Akt pathway plays in driving tumorogenesis or tumor proliferation in many cancers (71, 72). Activating mutations upstream of Akt in receptors like EGFR or downstream PI3K are frequently found in cancers, making these proteins important targets to inhibit in many cancers (71). However, we previously did not observe increased cellular proliferation with SC79 during acute (24-48 hrs) stimulation (44), and to our knowledge tumors, have not been reported in animal models in which SC79 has been examined (49-52). We hypothesize that transient pharmacological Akt activation in an acute infection setting will likely have very different effects compared with activating mutations that cause chronic Akt activation and which are often accompanied by other oncogenic mutations in parallel. However, for this reason, the use of SC79 still requires further *in vitro* and *in vivo* testing. However, our data here and from a previous study (44) suggest acute SC79 may have both anti-inflammatory and bactericidal benefits with limited cellular toxicity in a respiratory infection/topical delivery setting.

Methods

Reagents and Solutions

SC79, L-NAME, D-NAME, cPTIO, MK2206, LY294002, U73122, U73343, and colistin sulfate were from Cayman Chemical. API-2 was from Tocris. DAF-FM diacetate was from ThermoFisher Scientific. Unless specified below, all reagents were from MilliporeSigma. LDH assay kit (catalog no. ab65393) was from Abcam. *P. aeruginosa* flagellin (FLA-PA) was from InvivoGen. Stock solutions of hydrophobic compounds were made in DMSO at ≥1000x so that final DMSO concentrations were ≤0.1%. Vehicle control matched the highest DMSO concentration used in an experimental paradigm. Hank's balanced salt solution (HBSS) was used in all live cell imaging experiments and contained (in mM) 137 NaCl, 5 KCl, 0.4 KH_2PO_4, 0.3 Na_2HPO_4, 5.5 glucose, 1.8 $CaCl_2$, 1.5 $MgCl_2$, 20 HEPES, pH 7.4, supplemented with 1x MEM amino acids to provide a roughly physiological level of L-arginine for NO production.

Cell Culture

Primary human nasal epithelial cells were collected in accordance with The University of Pennsylvania guidelines regarding use of residual clinical material from patients undergoing sinonasal surgery at the University of Pennsylvania with institutional review board approval (#800614) and written informed consent from each patient in accordance with the U.S. Department of Health and Human Services code of federal regulation Title 45 CFR 46.116. Inclusion criteria were patients ≥18 years of age undergoing sinonasal surgery for sinonasal disease (CRS) or other procedures (e.g. trans-nasal approaches to the skull base). Exclusion criteria included history of systemic inheritable disease (e.g., granulomatosis with polyangiitis, cystic fibrosis, systemic immunodeficiencies) or use of antibiotics, oral corticosteroids, or anti-biologics (e.g. Xolair) within one month of surgery. Individuals ≤18 years of age, pregnant women, and cognitively impaired persons were not included. Tissue was transported to the lab in saline on ice and mucosal tissue was immediately removed for cell isolation.

Sinonasal epithelial cells were enzymatically dissociated and grown to confluence in proliferation medium (50% DMEM/Ham's F-12 plus 50% bronchial epithelial basal media [BEBM] plus Singlequot supplements [Lonza]) for 7 days (21). Confluent cells were dissociated and seeded on Corning transwells (0.33 cm^2, 0.4 μm pore size; transparent; Corning) coated with BSA, type I bovine collagen, and human fibronectin. When culture medium was removed from the upper compartment, basolateral media was changed to differentiation medium (1:1 DMEM:BEBM) containing hEGF (0.5 ng/ ml), epinephrine (5 ng/ml), BPE (0.13 mg/ml), hydrocortisone (0.5 ng/ml), insulin (5 ng/ml), triiodothyronine (6.5 ng/ml), and transferrin (0.5

ng/ml), supplemented with 100 U/ml penicillin, 100 g/ml streptomycin, 0.1 nM retinoic acid, and 2% NuSerum (BD Biosciences, San Jose, CA) from the Singlequot supplements as described (21). Cells were fed basolaterally with differentiation media for ~21 days prior to use. Primary ALI cultures were genotyped for *TAS2R38* AVI (non-functional) or PAV (functional) polymorphims as described.(21) Differentiation was verified based airway epithelial morphology (formation of motile cilia, goblet cells) and transepithelial electrical resistance, etc..

Primary human M0 macrophages were cultured as described (31) in RPMI2650 media with 10% human serum and 1x cell culture Pen/Strep. De-identified monocytes from healthy apheresis donors were obtained from the University of Pennsylvania Human Immunology core with written informed consent of every participant and institutional review board approval. Cells isolated from 10 different individuals were used. As all samples were de-identified for race, age, sex, etc., samples were used in a blinded fashion. Macrophages were differentiated by adherence culture for 12 days in 8-well chamber slides (CellVis) as described (31). Our prior studies suggest no differences in T2R responses among macrophages differentiated by adherence alone or by adherence plus M-CSF (31), and thus adherence only was used for these studies.

Live cell imaging of NO production

Primary human ALIs were loaded for 90 min with DAF-FM diacetate as previously described (21) in Hank's Balanced Salt solution (HBSS) buffered to pH 7.4 with 20 mM HEPES. Macrophages on glass chambered coverslips were loaded with 5 μM DAF-FM diacetate for 45 min as previously described (31). DAF-FM was imaged as previously described (21, 73) on a TS100 microscope (Nikon) with 10x 0.3 NA PlanFluor objective, Retiga R1 CCD camera, standard FITC/GFP filter set (Chroma), and XCite 110 LED illumination source. Images were acquired with the micromanager variant of ImageJ (74).

Immunofluorescence (IF) microscopy

IF was carried out as previously described (21). ALIs were fixed in 4% formaldehyde for 20 min at room temperature, followed by blocking and permeabilization in Dulbecco's phosphate buffered saline (DPBS) containing 1% bovine serum albumin (BSA) and 5% normal donkey serum (NDS) for blocking as well as 0.2% saponin and 0.3% triton X-100 for permeabilization for 1 hour at 4°C. Primary antibody incubation (1:100) was at 4°C overnight. Incubation with AlexaFluor (AF)-labeled antibodies (1:1000) was for 2 hours at 4°C. Transwell filters were removed from the plastic ring and mounted with Fluoroshield with DAPI (Abcam; Cambridge,

MA USA)). Images were taken on an Olympus Fluoview FV1000 confocal system with IX-73 microscope and 60x (1.4 NA) objective and analyzed in FIJI(75) using linear min/max adjustments. Anti-beta-tubulin IV (ab11315; mouse monoclonal; RRID:AB_297919) antibody was from Abcam. Donkey-raised, Alexa-Fluor-conjugated secondary antibodies (anti-rabbit AlexaFluor 546 [RRID:AB_2534016] and anti-mouse AlexaFluor 488 [RRID:AB_141607]) were from ThermoFisher Scientific.

Quantitative PCR

RNA was isolated from ALI cultures or stripped turbinate or polyp epithelium, as described previously (54), and qPCR was performed using TaqMan primers (Thermo Fisher Scientific) for IL8 and glyceraldehyde-3-phosphate dehydrogenase in separate reactions, and relative expression was calculated by calculated by means of the $2^{-\Delta\Delta Ct}$ method.

Bacteria culture

P. aeruginosa strains PAO-1 (ATCC 15692) and clinical CRS-isolates (Drs. N. Cohen and L. Chandler, Philadelphia VA Medical Center) (70) were grown in Luria broth (Gibco). For anti-bacterial assays, *P. aeruginosa* were grown to OD 0.1, centrifuged, and resuspended in 50% 0.9% saline supplemented with 0.5 mM glucose and 1 mM HEPES, pH 6.5. Nasal ALIs were washed 24 hrs prior to the assaywith antibiotic-free Ham's F12K media (ThermoFisher Scientific) basolaterally. 30 uL of bacteria saline solution was placed on the apical side of the ALI for 10 min, followed by aspiration of bulk ASL fluid. After 2 hrs at 37 °C, remaining bacteria were collected from the ALI by washing. Bacteria were live-dead stained with SYTO9 (live; green) and propidium iodide (dead; red) with BacLight Bacterial Viability Kit (ThermoFisher Scientific). Green/red fluorescence ratio was quantified in a Spark 10M (Tecan, Mannedorf, Switzerland; 485 nm excitation with 530 nm and 620 nm emission). CFU counting was done as previously described on LB plates with serial dilutions.(22, 70)

Phagocytosis assays

Phagocytosis assay were performed as described. (31) Macrophages were incubated in phenol red-free, low glucose DMEM with heat-killed FITC-labeled *Escherichia coli* at 250 µg/ml (strain K-12; reagents from Vybrant phagocytosis assay kit; ThermoFisher Scientific; Cat # E2861) (ThermoFisher Scientific) ± T2R agonist for 15 min at 37°C. Extracellular FITC was quenched with trypan blue per the manufacturer's instructions, and fluorescence was recorded on a Spark 10M plate reader (Tecan; 485 nm excitation, 535 nm emission). As phagocytosis is

negligible from 4 °C up to room temp,(31) we recorded fluorescence from living cells at room temperature immediately after the FITC-*E. coli*. For representative micrograph shown, macrophages on glass were incubated as above, and extracellular FITC was quenched with trypan blue and cells were washed ≥5x in PBS to remove residual extracellular FITC-*E. coli*. Remaining adherent MΦs were fixed in 4% formaldehyde (Electron Microscopy Sciences, Hatfield, PA) for 10 min followed by DAPI staining in mounting media (Fluoroshield with DAPI, Abcam). FITC-E. coli were then imaged using standard FITC filter set (Semrock, Rochester, NY) on an inverted Olympus IX-83 microscope with 20x (0.8 NA) objective, XCite 120LEDBoost illumination source, and Hammamatsu Orca Flash 4.0 sCMOS camera.

Phagocytosis assays were also carried out similarly using 125 µg/ml pHrodo red-labeled *S. aureus* (strain Wood 46; ThermoFisher Scientific, cat # A10010) (31). As pHrodo dyes only fluoresce when particles are internalized into low pH endosomes (previously demonstrated in (31)), this assay does not require washing or quenching of the extracellular pHrodo *S. aureus*. Macrophages were incubated with pHrodo-*S. aureus* for 30 min at 37°C as described (31) with excitation at 555 nm and emission at 595 nm measured on the Tecan Spark 10M plate reader. Background measurements were made using wells containing fluorescent *S. aureus* in the absence of macrophages. Representative images were taken as above except using a standard TRITC filter set (Semrock). Images shown for comparison were collected on the same day under identical conditions with identical min/max settings. No non-linear (e.g., gamma) adjustments were made to any images for either display or analysis.

Data analysis and statistics

Multiple comparisons were analyzed with one-way ANOVA with appropriate posttests: Bonferroni for pre-selected pairwise comparisons, Tukey-Kramer for comparing all values, or Dunnett's for comparing to control value. Asterisks (* and **) indicate $p < 0.05$ and $p < 0.01$, respectively; $p < 0.05$ was considered statistically significant. All data in bar graphs are shown as mean ± SEM with n derived from biological replicates (separate experiments conducted with different patient cells on different days). Raw unprocessed image data were analyzed in FIJI (75) and resulting numerical data were analyzed in Excel (Microsoft) and/or Prism (GraphPad software, La Jolla, CA). All data used to generate bar graphs and traces are available upon request.

Acknowledgements: This study was supported by NIH grants R01DC016308 (to R.J.L.) and R01AI167971 (to N.D.A., J.N.P., and R.J.L.). We thank J. Riley (University of Pennsylvania Perelman School of Medicine, Human Immunology Core) for primary human monocytes (supported by P30CA016520 and P30AI045008). We thank M. Victoria and J. Freund (University of Pennsylvania Perleman School of Medicine) for technical assistance. We thank B. Chen, N. Cohen, and L.E. Kuek (University of Pennsylvania Perelman School of Medicine) for assistance with isolation of patient nasal cells.

CRediT authorship contribution statement: Robert J. Lee: Conceptualization, Investigation, Methodology, Formal analysis, Writing – original draft, Writing – review & editing, Project administration, Funding acquisition. Nithin D. Adappa: Resources, Data curation, Project administration, Writing – review & editing, Funding acquisition. James N. Palmer: Resources, Data curation, Project administration, Writing – review & editing, Funding acquisition.

Figures

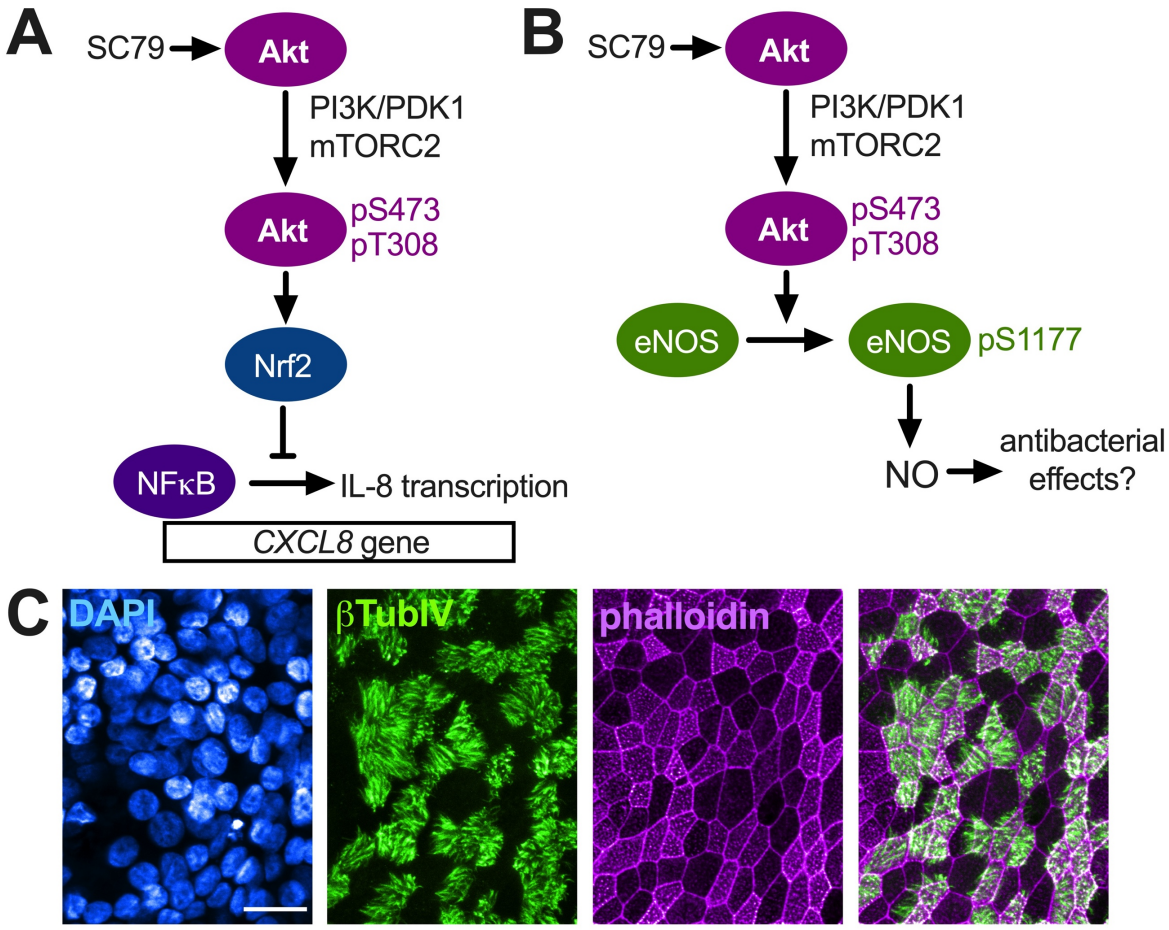

Figure 1: Small molecule Akt activator SC79 increases NO production in nasal epithelial air-liquid interface cultures (ALIs). (A) SC79 binds to Akt and promotes its phosphorylation and activation downstream of PI3 kinase (PI3K) and phosphoinositide-dependent protein kinase-1 (PDK-1) as well as mTOR Complex 2 (mTORC-2) at S473 and pT308. We previously showed that SC79 causes Akt-dependent increase in Nrf-2 levels in the nucleus that suppress NFκB transcription of IL-8 (44). **(B)** We also showed that SC79 induced Akt-dependent phosphorylation of endothelial nitric oxide synthase (eNOS) at pS1177 that stimulates nitric oxide (NO) production. We hypothesized that this may have antibacterial effects in nasal epithelial cells. **(C)** Effects of SC79 were tested in air-liquid interface (ALI) cultures of primary nasal epithelial cells, which form tight junctions (labeled with actin stain phalloidin, shown in magenta) and differentiated ciliated cells (shown by immunofluorescence of cilia-enriched β-tubulin isoform IV) and non-ciliated (goblet cells). Scale bar is 20 μm.

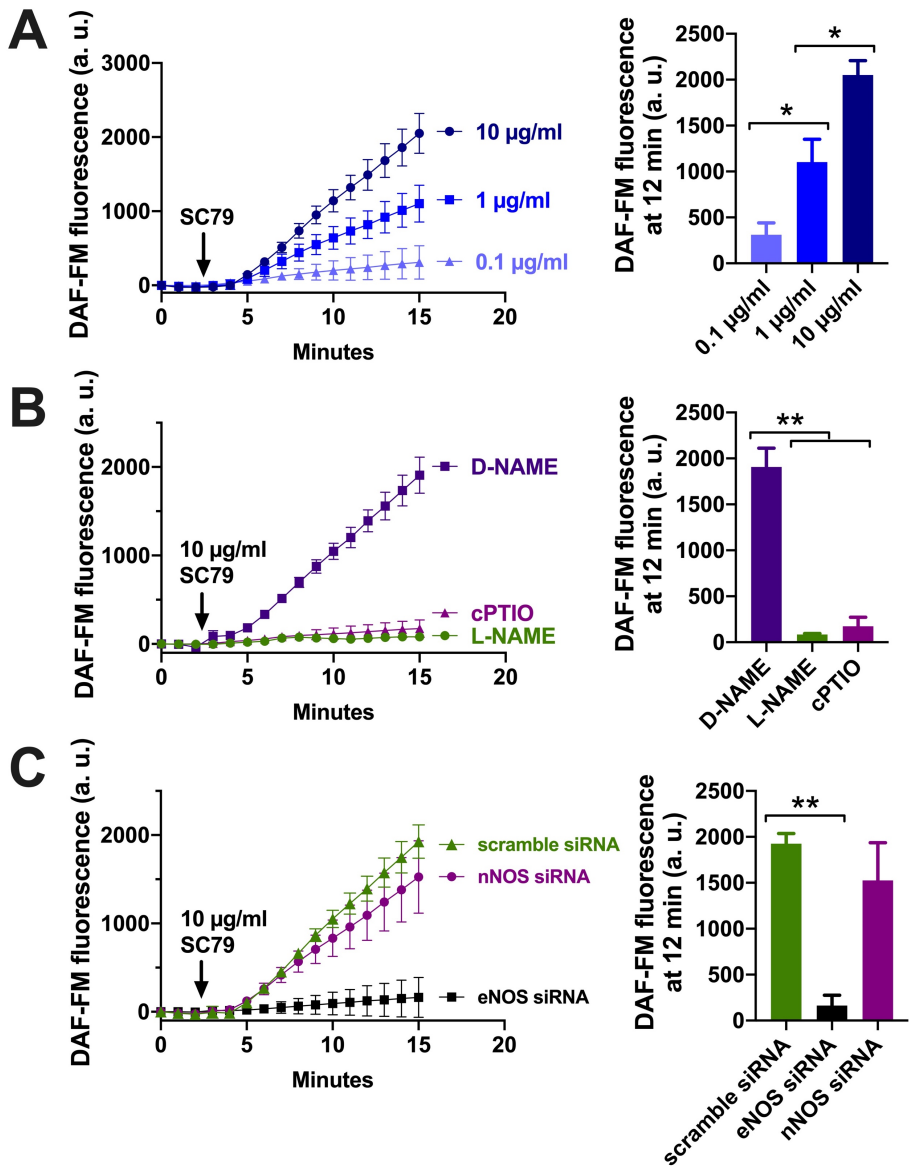

Figure 2: SC-79-induced NO production is dependent on eNOS activity. (A) Traces (left) and bar graph (right) of NO-sensitive dye DAF-FM in primary nasal ALIs confirming dose-dependent increase in DAF-FM fluorescence by SC79. SC79 activates Akt independent of other kinases (e.g., ERK) which may be activated during stimulation with receptor ligands such as EGF. Data from 4 independent expeirments using ALIs from different patients. Significance by one-way ANOVA with Bonferroni posttest; *$p<0.05$. **(B)** Traces (left) and bar graph (right) showing inhibition by NO scavenger cPTIO (10 µM) or NOS inhibitor L-NAME (45 min pre-treatment; 10 µM) but not inactive D-NAME (45 min pre-treatment; 10 µM); n = 4 independent experiments using ALIs from 4 separate patients. Significance by one-way ANOVA with Bonferroni posttest; **$p<0.01$. **(C)** Traces (left) and bar graph (right) showing inhibition by eNOS but not scramble or nNOS siRNA (treatment as described (76)); n = 4 independent experiments using ALIs from 4 separate patients. Significance by one-way ANOVA with Bonferroni posttest; **$p<0.01$.

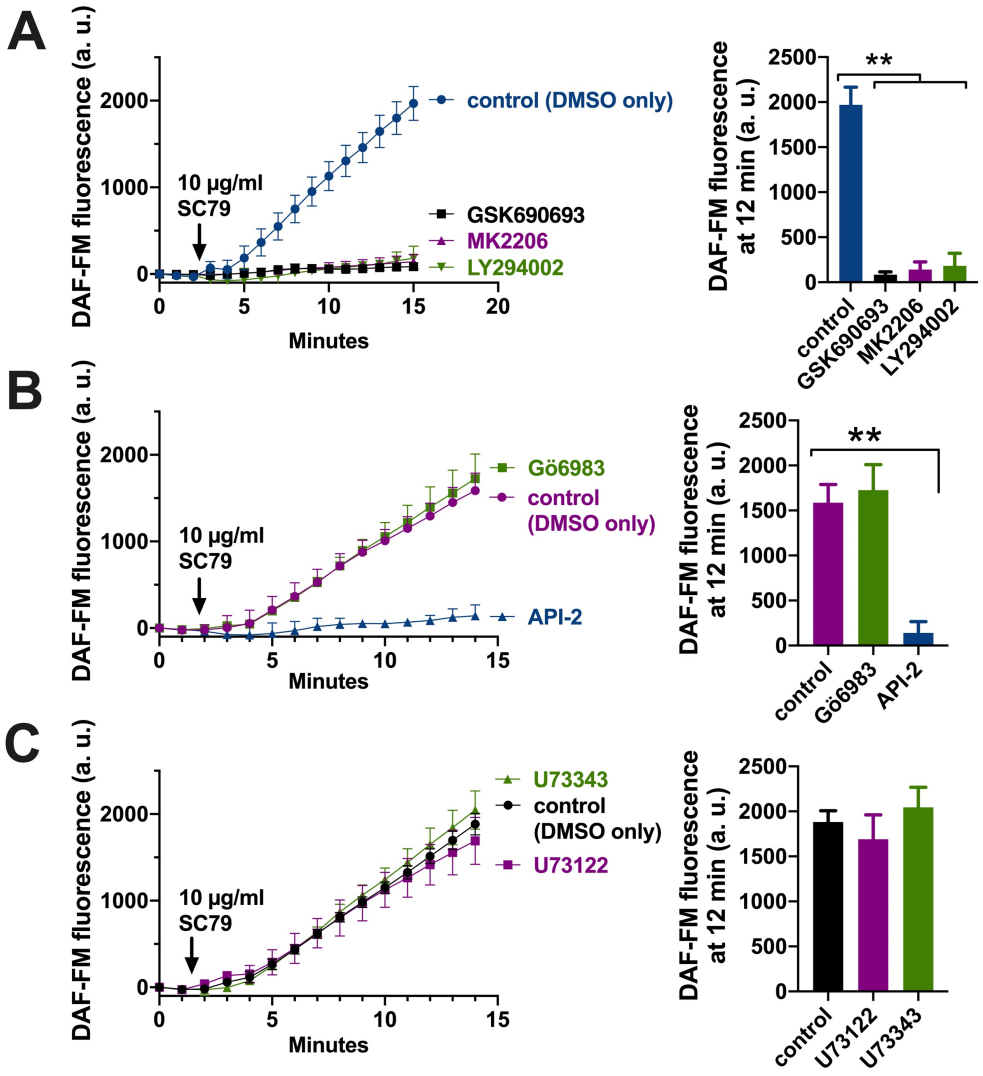

Figure 3: SC79 activation of eNOS requires Akt activity. (A) Trace (left) and bar graph (right) of DAF-FM fluorescence during stimulation with 10 µg/ml SC79 ± Akt inhibitor GSK6906932 (1 µM), Akt inhibitor MK2206 (1 µM), or LY294002 (1 µM). **(B)** Trace (left) and bar graph (right) of DAF-FM fluorescence during stimulation with 10 µg/ml SC79 in the presence of PKC inhibitor Gö6983 (1 µM) or Akt inhibitor API-2 (1 µM). **(C)** Trace (left) and bar graph (right) of DAF-FM fluorescence during stimluation with 10 µg/ml SC79 in the presence of PLC inhibitor U73122 (10 µM) or inactive analogue U73343 (10 µM). DMSO only was included in all control conditions. Pre-treatment with inhibitors was for 15 min prior to stimulation in the continued presence of inhibitor. All results from 3 independent experiments on different days using ALI from 3 different patients. Significance by one way ANOVA with Dunnett's posttest comparing all values to control.

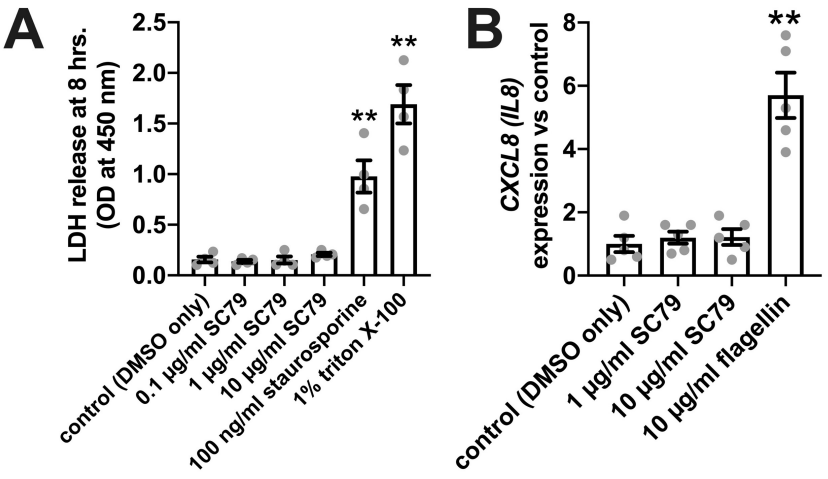

Figure 4: Lack of cytotoxic or inflammatory effects with acute exposure to SC79. (A) LDH release into cell culture media was measured via colorimetric assay. Staurosporine and triton X-100 were used as controls to induce apoptotic death (which is followed by secondary necrosis in the absence of phagocytic macrophages (77) and nonspecific lysis, respectively. No LDH release was observed with SC79. **(B)** IL-8 transcription was quantified by qPCR (normalized to GAPDH) after 24 hours stimulation with SC79 or TLR5 agonist flagellin. Each data point is an independent ALI from a different patient (n = 5 total ALIs). Significance by 1-way ANOVA with Dunnett posttest; ***p*<0.01.

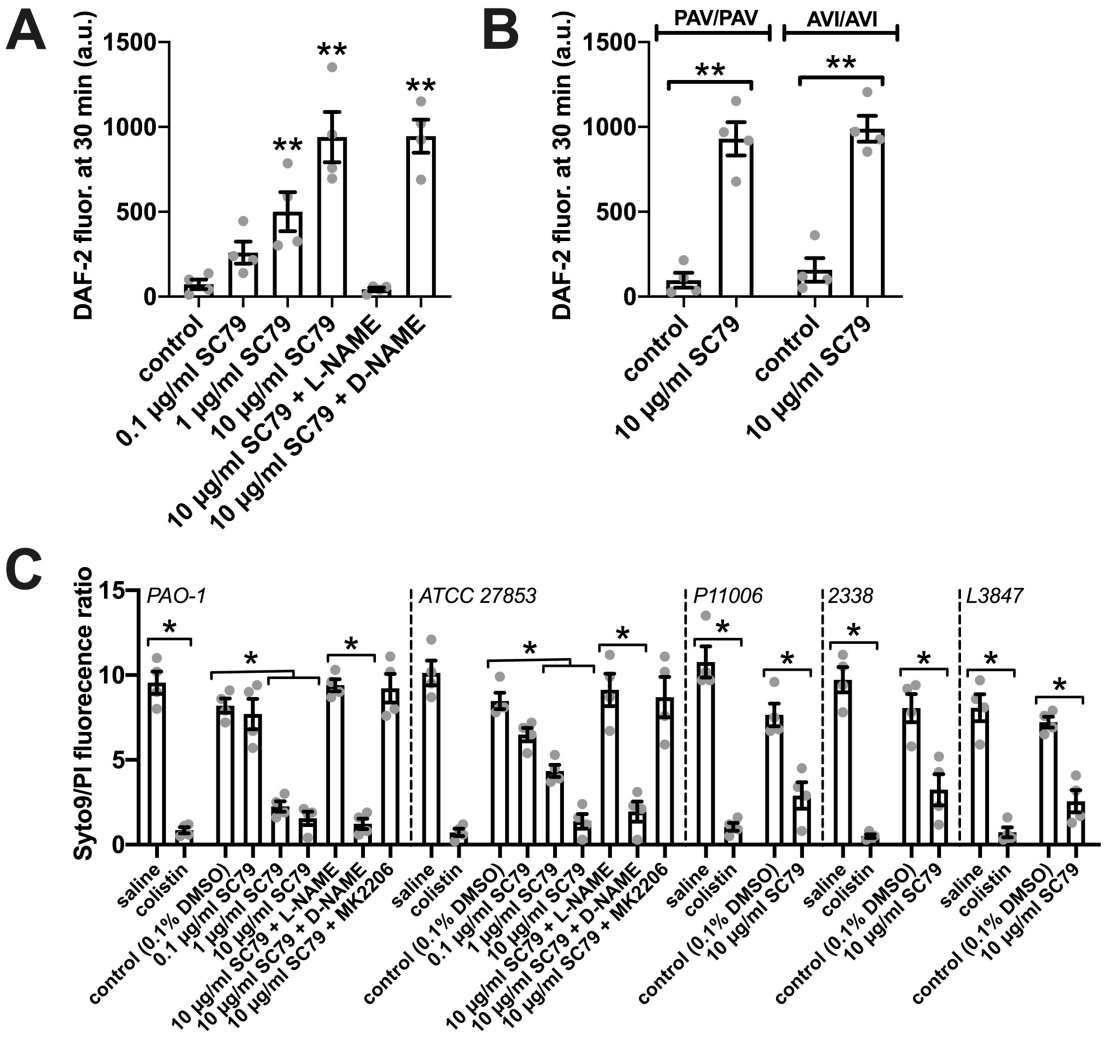

Figure 5: SC79 stimulates release of NO into the airway surface liquid with antibacterial effects. (A) Bar graph of fluorescence changes of cell impermeant DAF-2 overlayed on top of ALI cultures (as described (22)) showing dose-dependent increases with SC79 and inhibition by NOS inhibitor L-NAME but not inactive analogue D-NAME. Significance by one-way ANOVA comparing all values with control; **p<0.01. **(B)** DAF-2 measurement of ASL NO production was tested in TAS2R38 PAV/PAV (homozygous functional) vs AVI/AVI (homozygous non-functional) cultures. SC79 significantly increased DAF-2 fluorescence vs control in both genotypes; no difference was observed between SC79 stimulated PAV/PAV or AVI/AVI cultures. Significance by one-way ANOVA with Bonferroni posttest; **p<0.01. **(C)** Bar graph of Syto9/PI fluorescence from bacterial killing assay (as described (22, 25)) using AVI/AVI *TAS2R38* cultures showing less viable bacteria (lower Syto9/PI ratio) with SC79. Significances by one-way ANOVA with Bonferroni posttest.All results in *A-C* from 4 independent experiments on different days using ALIs from 4 different cultures.

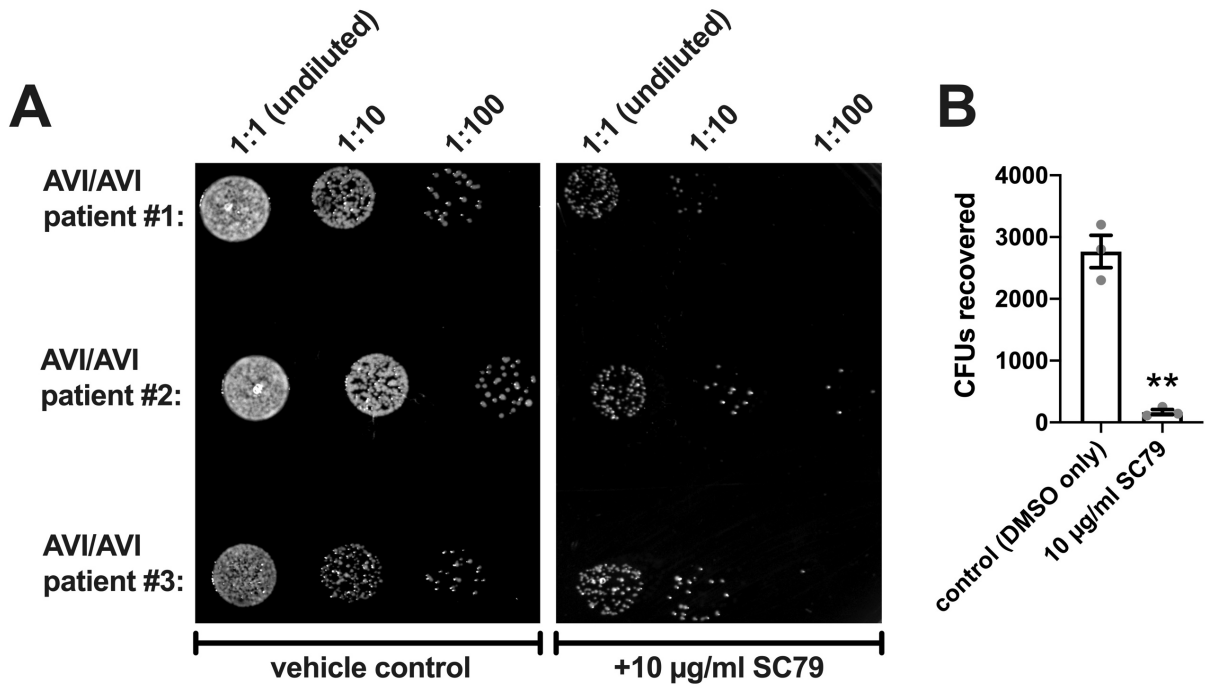

Figure 6: Verification of SC79 antimicrobial activity by colony forming unit (CFU) counting. (A) Bacteria recovered from nasal epithelial cultures (*TAS2R38* AVI/AVI) were collected, diluted in saline, and spotted on LB plates for manual CFU counting. **(B)** Quantification revealed a reduction in CFUs with SC79 treatment. Significance by Student's *t* test; $^{**}p<0.01$.

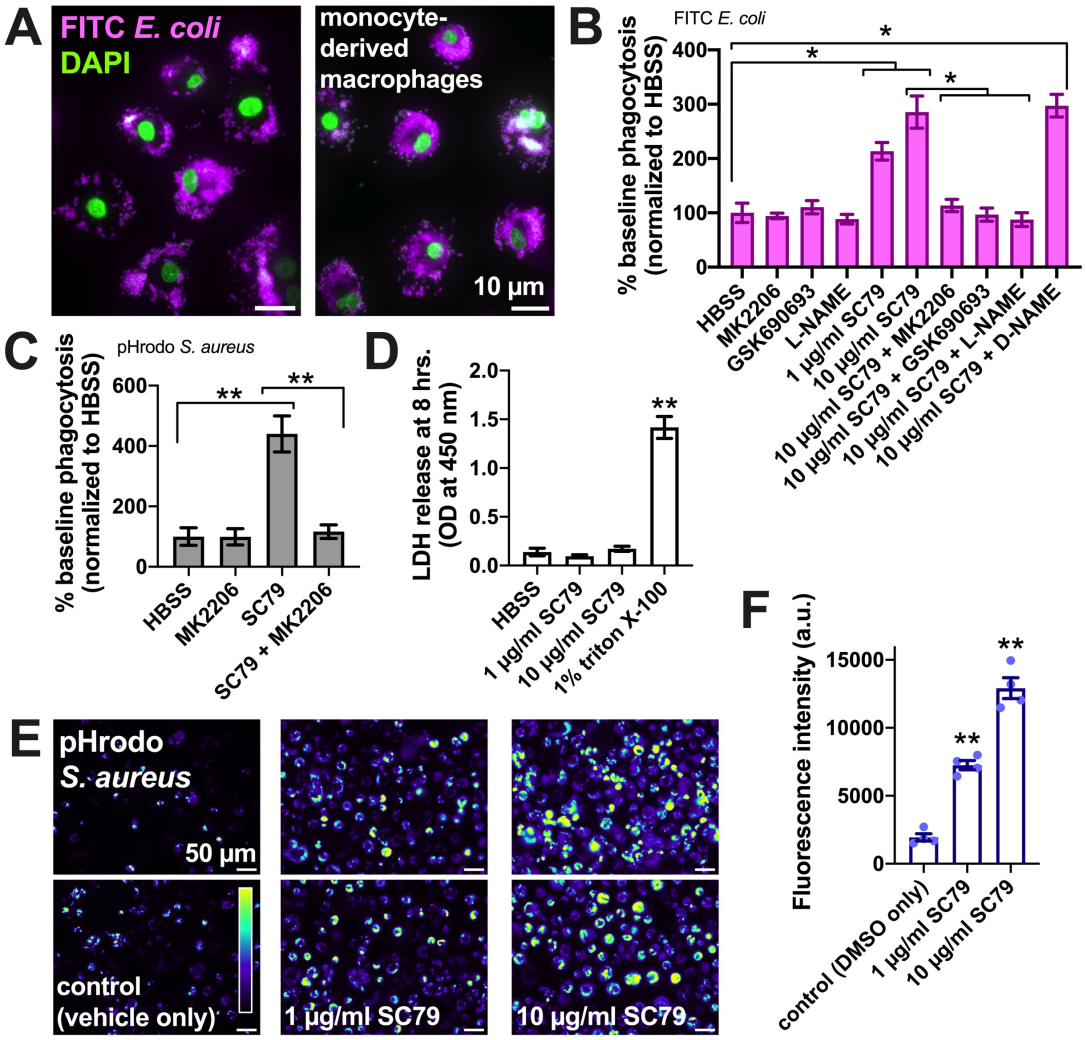

Figure 7: SC79 stimulates macrophage phagocytosis via Akt and NO signaling. (A) Images showing phagocytosis of FITC-labeled *E. coli* (magenta, DAPI nuclear stain in green) in primary human monocyte-derived macrophages, as described (22, 31). **(B)** FITC fluorescence (indicating macrophage phagocytosis) increased with SC79 treatment, which was blocked by Akt inhibitors MK2206 or GSK690693 and NOS inhibitor L-NAME. Significance by one-way ANOVA with Dunnett's posttest comparing all values to control; *$p<0.05$. Data are from 5 independent experiments using cells from 5 donors. **(C)** Phagocytosis of pHrodo S. aureus also increased with 10 µg/ml SC79 and was blocked by MK2206. Note that pHrodo only fluoresces in acid environments like the phagosome, confirming that internalization reflects phagocytosis. Data from 5 independent experiments using cells from 5 donors. Significance by one-way ANOVA with Bonferroni posttest; **$p<0.01$. **(D)** LDH release from macrophages was measured after 8 hours stimulation. Data from 4 independent experiments using cells from 4 donors. Significance by one-way ANOVA with Dunnett's posttest comparing all values to control; **$p<0.01$. **(E)** Microscope images of pHrodo *S. aureus* phagocytosed in macrophages. **(F)** Quantification of 4 independent experiments as shown in *E* confirms dose-dependent increase in phagocytosis with SC79. Significance by one-way ANOVA with Dunnett's posttest comparing all values to control; **$p<0.01$.

References

1. Workman AD, Carey RM, Kohanski MA, Kennedy DW, Palmer JN, Adappa ND, et al. Relative Susceptibility of Airway Organisms to Antimicrobial Effects of Nitric Oxide. *Int Forum Allergy Rhinol* (2017). doi: 10.1002/alr.21966.

2. Yu K, Mitchell C, Xing Y, Magliozzo RS, Bloom BR, Chan J. Toxicity of Nitrogen Oxides and Related Oxidants on Mycobacteria: M. Tuberculosis Is Resistant to Peroxynitrite Anion. *Tuber Lung Dis* (1999) 79(4):191-8. doi: 10.1054/tuld.1998.0203.

3. Marcinkiewicz J. Nitric Oxide and Antimicrobial Activity of Reactive Oxygen Intermediates. *Immunopharmacology* (1997) 37(1):35-41. Epub 1997/08/01. doi: S0162310996001683 [pii].

4. Fang FC. Perspectives Series: Host/Pathogen Interactions. Mechanisms of Nitric Oxide-Related Antimicrobial Activity. *J Clin Invest* (1997) 99(12):2818-25. Epub 1997/06/15. doi: 10.1172/JCI119473.

5. Wiegand SB, Traeger L, Nguyen HK, Rouillard KR, Fischbach A, Zadek F, et al. Antimicrobial Effects of Nitric Oxide in Murine Models of Klebsiella Pneumonia. *Redox Biol* (2021) 39:101826. Epub 2020/12/23. doi: 10.1016/j.redox.2020.101826.

6. Wink DA, Hines HB, Cheng RY, Switzer CH, Flores-Santana W, Vitek MP, et al. Nitric Oxide and Redox Mechanisms in the Immune Response. *J Leukoc Biol* (2011) 89(6):873-91. doi: 10.1189/jlb.1010550.

7. Akerstrom S, Mousavi-Jazi M, Klingstrom J, Leijon M, Lundkvist A, Mirazimi A. Nitric Oxide Inhibits the Replication Cycle of Severe Acute Respiratory Syndrome Coronavirus. *J Virol* (2005) 79(3):1966-9. Epub 2005/01/15. doi: 10.1128/JVI.79.3.1966-1969.2005.

8. Akerstrom S, Gunalan V, Keng CT, Tan YJ, Mirazimi A. Dual Effect of Nitric Oxide on Sars-Cov Replication: Viral Rna Production and Palmitoylation of the S Protein Are Affected. *Virology* (2009) 395(1):1-9. Epub 2009/10/06. doi: 10.1016/j.virol.2009.09.007.

9. Akaberi D, Krambrich J, Ling J, Luni C, Hedenstierna G, Jarhult JD, et al. Mitigation of the Replication of Sars-Cov-2 by Nitric Oxide in Vitro. *Redox Biol* (2020) 37:101734. Epub 2020/10/03. doi: 10.1016/j.redox.2020.101734.

10. Hedenstierna G, Chen L, Hedenstierna M, Lieberman R, Fine DH. Nitric Oxide Dosed in Short Bursts at High Concentrations May Protect against Covid 19. *Nitric Oxide* (2020) 103:1-3. Epub 2020/06/27. doi: 10.1016/j.niox.2020.06.005.

11. Sherman TS, Chen Z, Yuhanna IS, Lau KS, Margraf LR, Shaul PW. Nitric Oxide Synthase Isoform Expression in the Developing Lung Epithelium. *Am J Physiol* (1999) 276(2 Pt 1):L383-90.

12. Shaul PW, North AJ, Wu LC, Wells LB, Brannon TS, Lau KS, et al. Endothelial Nitric Oxide Synthase Is Expressed in Cultured Human Bronchiolar Epithelium. *J Clin Invest* (1994) 94(6):2231-6. doi: 10.1172/JCI117585.

13. German Z, Chambliss KL, Pace MC, Arnet UA, Lowenstein CJ, Shaul PW. Molecular Basis of Cell-Specific Endothelial Nitric-Oxide Synthase Expression in Airway Epithelium. *J Biol Chem* (2000) 275(11):8183-9.

14. Carey RM, Adappa ND, Palmer JN, Lee RJ. Neuropeptide Y Reduces Nasal Epithelial T2r Bitter Taste Receptor–Stimulated Nitric Oxide Production. *Nutrients* (2021) 13(10):3392.

15. Stout SL, Wyatt TA, Adams JJ, Sisson JH. Nitric Oxide-Dependent Cilia Regulatory Enzyme Localization in Bovine Bronchial Epithelial Cells. *J Histochem Cytochem* (2007) 55(5):433-42. Epub 2007/01/24. doi: jhc.6A7089.2007 [pii] 10.1369/jhc.6A7089.2007.

16. Sisson JH, Pavlik JA, Wyatt TA. Alcohol Stimulates Ciliary Motility of Isolated Airway Axonemes through a Nitric Oxide, Cyclase, and Cyclic Nucleotide-Dependent Kinase Mechanism. *Alcohol Clin Exp Res* (2009) 33(4):610-6. Epub 2009/02/03. doi: ACER875 [pii] 10.1111/j.1530-0277.2008.00875.x.

17. Sisson JH, May K, Wyatt TA. Nitric Oxide-Dependent Ethanol Stimulation of Ciliary Motility Is Linked to Camp-Dependent Protein Kinase (Pka) Activation in Bovine Bronchial Epithelium. *Alcohol Clin Exp Res* (1999) 23(9):1528-33. Epub 1999/10/08. doi: 00000374-199909000-00016 [pii].

18. Simet SM, Pavlik JA, Sisson JH. Proteomic Analysis of Bovine Axonemes Exposed to Acute Alcohol: Role of Endothelial Nitric Oxide Synthase and Heat Shock Protein 90 in Cilia Stimulation. *Alcohol Clin Exp Res* (2013) 37(4):609-15. Epub 2012/10/20. doi: 10.1111/acer.12014.

19. Dudzinski DM, Michel T. Life History of Enos: Partners and Pathways. *Cardiovasc Res* (2007) 75(2):247-60. Epub 2007/05/01. doi: 10.1016/j.cardiores.2007.03.023.

20. Forstermann U, Sessa WC. Nitric Oxide Synthases: Regulation and Function. *Eur Heart J* (2012) 33(7):829-37, 37a-37d. doi: 10.1093/eurheartj/ehr304.

21. Carey RM, Adappa ND, Palmer JN, Lee RJ. Neuropeptide Y Reduces Nasal Epithelial T2r Bitter Taste Receptor-Stimulated Nitric Oxide Production. *Nutrients* (2021) 13(10). Epub 2021/10/24. doi: 10.3390/nu13103392.

22. Carey RM, Hariri BM, Adappa ND, Palmer JN, Lee RJ. Hsp90 Modulates T2r Bitter Taste Receptor Nitric Oxide Production and Innate Immune Responses in Human Airway Epithelial Cells and Macrophages. *Cells* (2022) 11(9). Epub 2022/05/15. doi: 10.3390/cells11091478.

23. Margolskee RF. Molecular Mechanisms of Bitter and Sweet Taste Transduction. *J Biol Chem* (2002) 277(1):1-4. Epub 2001/11/07. doi: 10.1074/jbc.R100054200.

24. Shah AS, Ben-Shahar Y, Moninger TO, Kline JN, Welsh MJ. Motile Cilia of Human Airway Epithelia Are Chemosensory. *Science* (2009) 325(5944):1131-4. Epub 2009/07/25. doi: 1173869 [pii] 10.1126/science.1173869.

25. Lee RJ, Xiong G, Kofonow JM, Chen B, Lysenko A, Jiang P, et al. T2r38 Taste Receptor Polymorphisms Underlie Susceptibility to Upper Respiratory Infection. *J Clin Invest* (2012) 122(11):4145-59.

26. Hariri BM, McMahon DB, Chen B, Freund JR, Mansfield CJ, Doghramji LJ, et al. Flavones Modulate Respiratory Epithelial Innate Immunity: Anti-Inflammatory Effects and Activation of the T2r14 Receptor. *J Biol Chem* (2017) 292(20):8484-97. Epub Apr 3. doi: 10.1074/jbc.M116.771949.

27. Freund JR, Mansfield CJ, Doghramji LJ, Adappa ND, Palmer JN, Kennedy DW, et al. Activation of Airway Epithelial Bitter Taste Receptors by Pseudomonas Aeruginosa Quinolones Modulates Calcium, Cyclic-Amp, and Nitric Oxide Signaling. *J Biol Chem* (2018) 293(25):9824-40. Epub 2018/05/12. doi: 10.1074/jbc.RA117.001005.

28. Carey RM, Lee RJ. Taste Receptors in Upper Airway Innate Immunity. *Nutrients* (2019) 11(9). Epub 2019/08/31. doi: 10.3390/nu11092017.

29. Lee RJ, Chen B, Redding KM, Margolskee RF, Cohen NA. Mouse Nasal Epithelial Innate Immune Responses to Pseudomonas Aeruginosa Quorum-Sensing Molecules Require Taste Signaling Components. *Innate Immun* (2014) 20(6):606-17. Epub 2013/09/21. doi: 10.1177/1753425913503386.

30. Lee RJ, Cohen NA. The Emerging Role of the Bitter Taste Receptor T2r38 in Upper Respiratory Infection and Chronic Rhinosinusitis. *Am J Rhinol Allergy* (2013) 27(4):283-6. Epub 2013/07/26. doi: 10.2500/ajra.2013.27.3911.

31. Gopallawa I, Freund JR, Lee RJ. Bitter Taste Receptors Stimulate Phagocytosis in Human Macrophages through Calcium, Nitric Oxide, and Cyclic-Gmp Signaling. *Cell Mol Life Sci* (2021) 78(1):271-86. Epub 2020/03/17. doi: 10.1007/s00018-020-03494-y.

32. Adappa ND, Zhang Z, Palmer JN, Kennedy DW, Doghramji L, Lysenko A, et al. The Bitter Taste Receptor T2r38 Is an Independent Risk Factor for Chronic Rhinosinusitis Requiring Sinus Surgery. *Int Forum Allergy Rhinol* (2014) 4(1):3-7. Epub 2013/12/05. doi: 10.1002/alr.21253.

33. Adappa ND, Howland TJ, Palmer JN, Kennedy DW, Doghramji L, Lysenko A, et al. Genetics of the Taste Receptor T2r38 Correlates with Chronic Rhinosinusitis Necessitating Surgical Intervention. *Int Forum Allergy Rhinol* (2013) 3(3):184-7.

34. Adappa ND, Farquhar D, Palmer JN, Kennedy DW, Doghramji L, Morris SA, et al. Tas2r38 Genotype Predicts Surgical Outcome in Nonpolypoid Chronic Rhinosinusitis. *Int Forum Allergy Rhinol* (2015). doi: 10.1002/alr.21666.

35. Mfuna Endam L, Filali-Mouhim A, Boisvert P, Boulet LP, Bosse Y, Desrosiers M. Genetic Variations in Taste Receptors Are Associated with Chronic Rhinosinusitis: A Replication Study. *Int Forum Allergy Rhinol* (2014) 4(3):200-6. Epub 2014/01/15. doi: 10.1002/alr.21275.

36. Dzaman K, Zagor M, Sarnowska E, Krzeski A, Kantor I. The Correlation of Tas2r38 Gene Variants with Higher Risk for Chronic Rhinosinusitis in Polish Patients. *Otolaryngol Pol* (2016) 70(5):13-8. doi: 10.5604/00306657.1209438.

37. Rom DI, Christensen JM, Alvarado R, Sacks R, Harvey RJ. The Impact of Bitter Taste Receptor Genetics on Culturable Bacteria in Chronic Rhinosinusitis. *Rhinology* (2017). doi: 10.4193/Rhin16.181.

38. Castaldo A, Cernera G, Iacotucci P, Cimbalo C, Gelzo M, Comegna M, et al. Tas2r38 Is a Novel Modifier Gene in Patients with Cystic Fibrosis. *Sci Rep* (2020) 10(1):5806. Epub 2020/04/04. doi: 10.1038/s41598-020-62747-9.

39. Adappa ND, Workman AD, Hadjiliadis D, Dorgan DJ, Frame D, Brooks S, et al. T2r38 Genotype Is Correlated with Sinonasal Quality of Life in Homozygous Deltaf508 Cystic Fibrosis Patients. *Int Forum Allergy Rhinol* (2016) 6(4):356-61. doi: 10.1002/alr.21675.

40. Rujanavej V, Soudry E, Banaei N, Baron EJ, Hwang PH, Nayak JV. Trends in Incidence and Susceptibility among Methicillin-Resistant Staphylococcus Aureus Isolated from Intranasal Cultures Associated with Rhinosinusitis. *Am J Rhinol Allergy* (2013) 27(2):134-7. Epub 2013/04/09. doi: 10.2500/ajra.2013.27.3858.

41. Marcinkiewicz J, Strus M, Pasich E. Antibiotic Resistance: A "Dark Side" of Biofilmassociated Chronic Infections. *Pol Arch Med Wewn* (2013) 123(6):309-13. Epub 2013/07/06.

42. Manes RP, Batra PS. Bacteriology and Antibiotic Resistance in Chronic Rhinosinusitis. *Facial Plast Surg Clin North Am* (2012) 20(1):87-91. Epub 2011/11/22. doi: 10.1016/j.fsc.2011.10.010.

43. Kingdom TT, Swain RE, Jr. The Microbiology and Antimicrobial Resistance Patterns in Chronic Rhinosinusitis. *Am J Otolaryngol* (2004) 25(5):323-8. Epub 2004/08/31. doi: S0196070904000341 [pii].

44. Gopallawa I, Kuek LE, Adappa ND, Palmer JN, Lee RJ. Small-Molecule Akt-Activation in Airway Cells Induces No Production and Reduces Il-8 Transcription through Nrf-2. *Respir Res* (2021) 22(1):267. Epub 2021/10/21. doi: 10.1186/s12931-021-01865-y.

45. Toker A, Marmiroli S. Signaling Specificity in the Akt Pathway in Biology and Disease. *Adv Biol Regul* (2014) 55:28-38. Epub 2014/05/06. doi: 10.1016/j.jbior.2014.04.001.

46. Manning BD, Toker A. Akt/Pkb Signaling: Navigating the Network. *Cell* (2017) 169(3):381-405. Epub 2017/04/22. doi: 10.1016/j.cell.2017.04.001.

47. Staal SP, Hartley JW, Rowe WP. Isolation of Transforming Murine Leukemia Viruses from Mice with a High Incidence of Spontaneous Lymphoma. *Proc Natl Acad Sci U S A* (1977) 74(7):3065-7. Epub 1977/07/01. doi: 10.1073/pnas.74.7.3065.

48. Jo H, Mondal S, Tan D, Nagata E, Takizawa S, Sharma AK, et al. Small Molecule-Induced Cytosolic Activation of Protein Kinase Akt Rescues Ischemia-Elicited Neuronal Death. *Proc Natl Acad Sci U S A* (2012) 109(26):10581-6. Epub 2012/06/13. doi: 10.1073/pnas.1202810109.

49. Li ST, Chen NN, Qiao YB, Zhu WL, Ruan JW, Zhou XZ. Sc79 Rescues Osteoblasts from Dexamethasone Though Activating Akt-Nrf2 Signaling. *Biochem Biophys Res Commun* (2016) 479(1):54-60. Epub 2016/09/11. doi: 10.1016/j.bbrc.2016.09.027.

50. Xu Y, Gao YW, Yang Y. Sc79 Protects Dopaminergic Neurons from Oxidative Stress. *Oncotarget* (2018) 9(16):12639-48. Epub 2018/03/22. doi: 10.18632/oncotarget.23538.

51. Zhang D, Zhang H, Hao S, Yan H, Zhang Z, Hu Y, et al. Akt Specific Activator Sc79 Protects against Early Brain Injury Following Subarachnoid Hemorrhage. *ACS Chem Neurosci* (2016) 7(6):710-8. Epub 2016/03/18. doi: 10.1021/acschemneuro.5b00306.

52. Jing ZT, Liu W, Xue CR, Wu SX, Chen WN, Lin XJ, et al. Akt Activator Sc79 Protects Hepatocytes from Tnf-Alpha-Mediated Apoptosis and Alleviates D-Gal/Lps-Induced Liver Injury. *Am J Physiol Gastrointest Liver Physiol* (2019) 316(3):G387-G96. Epub 2019/01/11. doi: 10.1152/ajpgi.00350.2018.

53. Kuek LE, Lee RJ. First Contact: The Role of Respiratory Cilia in Host-Pathogen Interactions in the Airways. *Am J Physiol Lung Cell Mol Physiol* (2020) 319(4):L603-L19. Epub 2020/08/14. doi: 10.1152/ajplung.00283.2020.

54. Carey RM, Freund JR, Hariri BM, Adappa ND, Palmer JN, Lee RJ. Polarization of Protease-Activated Receptor 2 (Par-2) Signaling Is Altered During Airway Epithelial Remodeling and Deciliation. *J Biol Chem* (2020) 295(19):6721-40. Epub 2020/04/04. doi: 10.1074/jbc.RA120.012710.

55. Belchamber KBR, Donnelly LE. Macrophage Dysfunction in Respiratory Disease. *Results Probl Cell Differ* (2017) 62:299-313. Epub 2017/04/30. doi: 10.1007/978-3-319-54090-0_12.

56. Fokkens WJ, Scheeren RA. Upper Airway Defence Mechanisms. *Paediatr Respir Rev* (2000) 1(4):336-41. doi: 10.1053/prrv.2000.0073.

57. Parker D, Prince A. Innate Immunity in the Respiratory Epithelium. *Am J Respir Cell Mol Biol* (2011) 45(2):189-201. Epub 2011/02/19. doi: 2011-0011RT [pii] 10.1165/rcmb.2011-0011RT.

58. Stevens WW, Lee RJ, Schleimer RP, Cohen NA. Chronic Rhinosinusitis Pathogenesis. *J Allergy Clin Immunol* (2015) 136(6):1442-53. doi: 10.1016/j.jaci.2015.10.009.

59. Spellberg B, Bartlett JG, Gilbert DN. The Future of Antibiotics and Resistance. *N Engl J Med* (2013) 368(4):299-302. doi: 10.1056/NEJMp1215093.

60. Bhattacharyya N, Kepnes LJ. Assessment of Trends in Antimicrobial Resistance in Chronic Rhinosinusitis. *Ann Otol Rhinol Laryngol* (2008) 117(6):448-52. Epub 2008/07/24.

61. Genoway KA, Philpott CM, Javer AR. Pathogen Yield and Antimicrobial Resistance Patterns of Chronic Rhinosinusitis Patients Presenting to a Tertiary Rhinology Centre. *J Otolaryngol Head Neck Surg* (2011) 40(3):232-7. Epub 2011/04/27.

62. Di Pietro C, Zhang PX, O'Rourke TK, Murray TS, Wang L, Britto CJ, et al. Ezrin Links Cftr to Tlr4 Signaling to Orchestrate Anti-Bacterial Immune Response in Macrophages. *Sci Rep* (2017) 7(1):10882. Epub 2017/09/09. doi: 10.1038/s41598-017-11012-7.

63. Pourrajab F, Yazdi MB, Zarch MB, Zarch MB, Hekmatimoghaddam S. Cross Talk of the First-Line Defense Tlrs with Pi3k/Akt Pathway, in Preconditioning Therapeutic Approach. *Mol Cell Ther* (2015) 3:4. doi: 10.1186/s40591-015-0041-7.

64. Jardeleza C, Thierry B, Rao S, Rajiv S, Drilling A, Miljkovic D, et al. An in Vivo Safety and Efficacy Demonstration of a Topical Liposomal Nitric Oxide Donor Treatment for Staphylococcus Aureus Biofilm-Associated Rhinosinusitis. *Transl Res* (2015) 166(6):683-92. Epub 2015/07/15. doi: 10.1016/j.trsl.2015.06.009.

65. Jardeleza C, Rao S, Thierry B, Gajjar P, Vreugde S, Prestidge CA, et al. Liposome-Encapsulated Ismn: A Novel Nitric Oxide-Based Therapeutic Agent against Staphylococcus Aureus Biofilms. *PLoS One* (2014) 9(3):e92117. Epub 2014/03/25. doi: 10.1371/journal.pone.0092117.

66. Lin C, Civantos AM, Arnold M, Stevens EM, Cowart BJ, Colquitt LR, et al. Divergent Bitter and Sweet Taste Perception Intensity in Chronic Rhinosinusitis Patients. *Int Forum Allergy Rhinol* (2020). Epub 2020/08/28. doi: 10.1002/alr.22686.

67. Adappa ND, Truesdale CM, Workman AD, Doghramji L, Mansfield C, Kennedy DW, et al. Correlation of T2r38 Taste Phenotype and in Vitro Biofilm Formation from Nonpolypoid Chronic Rhinosinusitis Patients. *Int Forum Allergy Rhinol* (2016) 6(8):783-91. doi: 10.1002/alr.21803.

68. Adappa ND, Farquhar D, Palmer JN, Kennedy DW, Doghramji L, Morris SA, et al. Tas2r38 Genotype Predicts Surgical Outcome in Nonpolypoid Chronic Rhinosinusitis. *Int Forum Allergy Rhinol* (2015) 6(1):25-33. doi: 10.1002/alr.21666.

69. Workman AD, Maina IW, Brooks SG, Kohanski MA, Cowart BJ, Mansfield C, et al. The Role of Quinine-Responsive T2rs in Airway Immune Defense and Chronic Rhinosinusitis. *Front Immunol* (2018) 9:624. Epub 13 Mar 2018. doi: doi: 10.3389/fimmu.2018.00624.

70. Kuek LE, McMahon DB, Ma RZ, Miller ZA, Jolivert JF, Adappa ND, et al. Cilia Stimulatory and Antibacterial Activities of T2r Bitter Taste Receptor Agonist Diphenhydramine: Insights into Repurposing Bitter Drugs for Nasal Infections. *Pharmaceuticals (Basel)* (2022) 15(4). Epub 2022/04/24. doi: 10.3390/ph15040452.

71. Hoxhaj G, Manning BD. The Pi3k-Akt Network at the Interface of Oncogenic Signalling and Cancer Metabolism. *Nat Rev Cancer* (2020) 20(2):74-88. Epub 2019/11/07. doi: 10.1038/s41568-019-0216-7.

72. Gopallawa I, Lee RJ. Targeting the Phosphoinositide-3-Kinase/Protein Kinase B Pathway in Airway Innate Immunity. *World J Biol Chem* (2020) 11(2):30-51. Epub 2020/10/08. doi: 10.4331/wjbc.v11.i2.30.

73. Carey RM, McMahon DB, Miller ZA, Kim T, Rajasekaran K, Gopallawa I, et al. T2r Bitter Taste Receptors Regulate Apoptosis and May Be Associated with Survival in Head and Neck Squamous Cell Carcinoma. *Mol Oncol* (2021). Epub 2021/10/31. doi: 10.1002/1878-0261.13131.

74. Edelstein A, Amodaj N, Hoover K, Vale R, Stuurman N. Computer Control of Microscopes Using Micromanager. *Curr Protoc Mol Biol* (2010) Chapter 14:Unit14 20. Epub 2010/10/05. doi: 10.1002/0471142727.mb1420s92.

75. Schindelin J, Arganda-Carreras I, Frise E, Kaynig V, Longair M, Pietzsch T, et al. Fiji: An Open-Source Platform for Biological-Image Analysis. *Nat Methods* (2012) 9(7):676-82. doi: 10.1038/nmeth.2019.

76. Bartman CM, Stelzig KE, Linden DR, Prakash YS, Chiarella SE. Passive Sirna Transfection Method for Gene Knockdown in Air-Liquid Interface Airway Epithelial Cell Cultures. *Am J Physiol Lung Cell Mol Physiol* (2021) 321(1):L280-L6. Epub 2021/05/27. doi: 10.1152/ajplung.00122.2021.

77. Silva MT. Secondary Necrosis: The Natural Outcome of the Complete Apoptotic Program. *FEBS Lett* (2010) 584(22):4491-9. Epub 2010/10/27. doi: 10.1016/j.febslet.2010.10.046.